

## Crystal Structure of Human DT-diaphorase: A Model for Interaction with the Cytotoxic Prodrug 5-(Aziridin-1-yl)-2,4-dinitrobenzamide (CB1954)

Jane V. Skelly,<sup>†</sup> Mark R. Sanderson,<sup>‡</sup> David A. Suter,<sup>†</sup> Ulrich Baumann,<sup>†</sup> Martin A. Read,<sup>†</sup> David S. J. Gregory,<sup>†</sup> Matthew Bennett,<sup>‡</sup> Stephen M. Hobbs,<sup>§</sup> and Stephen Neidle<sup>\*†</sup>

CRC Biomolecular Structure Unit and CRC Centre for Cancer Therapeutics, The Institute of Cancer Research, Cotswold Road, Sutton, Surrey SM2 5NG, U.K., and Randall Institute, Kings College London, 26-29 Drury Lane, London WC2B 5RL, U.K.

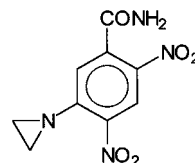
Received April 20, 1999

The crystal structure of human DT-diaphorase (NAD(P)H oxidoreductase (quinone); EC 1.6.99.2) has been determined to 2.3 Å resolution. There are only minor differences in shape and volume between the active sites of the rat and human enzymes and in the hydrophobic environment in the vicinity of the substrate. The isoalloxazine ring of the bound FAD is more buried in the human structure. Molecular modeling was used to examine optimal positions for the antitumor prodrug CB1954 (5-(aziridin-1-yl)-2,4-dinitrobenzamide) in both the human and rat enzyme active sites. This suggests that the position of CB1954 in the active site of the human enzyme is very similar to that in the rat, although there are detailed differences in the predicted patterns of hydrogen bonding between side chains and the drug. Some of the differences are a consequence of the shift in position for the FAD molecule and may contribute to the observed differences in rate of the two-electron reduction of CB1954.

### Introduction

DT-diaphorase (NAD(P)H oxidoreductase (quinone); EC 1.6.99.2) is an important detoxifying enzyme that is constitutively expressed in a variety of tissues, with particularly high levels in liver, kidney, and the gastrointestinal tract.<sup>1,2</sup> It catalyzes an obligatory two-electron reduction of a range of quinones and quinonoid compounds. High levels of DT-diaphorase activity are induced when cells are challenged by a variety of potentially carcinogenic and mutagenic compounds,<sup>3</sup> and there is substantial evidence for increased levels of activity in non-small-cell lung and colon carcinomas.<sup>4</sup> Several cytotoxic antitumor quinones, including the mitomycins, anthracyclines, and aziridinylbenzoquinones, are bioactivated by DT-diaphorase<sup>5</sup> to generate reactive intermediates which can undergo nucleophilic additions with DNA, resulting in single-strand breaks. It can also reduce nitrobenzene-containing compounds such as the antitumor prodrug 5-(aziridin-1-yl)-2,4-dinitrobenzamide (CB1954) (Chart 1) to form a cytotoxic interstrand cross-linking agent by reduction of its 4-nitro group.<sup>6</sup> Cells expressing high levels of DT-diaphorase are more sensitive to drug treatment.<sup>7,8</sup> DT-diaphorase is a tightly associated physiological dimer of identical subunits, each comprising 273 amino acids.<sup>9,10</sup> Each monomer contains a noncovalently bound FAD prosthetic group that is essential for catalytic activity. There are 37 amino acid differences between the rat and human enzymes (Figure 1). The two-domain structure for the monomer proposed on the basis of proteolytic digestion studies<sup>11</sup> was confirmed by the 2.1 Å resolution X-ray structure of the rat enzyme.<sup>12</sup> Crystal

Chart 1. Structure of CB1954



structures of two different complexes of the rat liver enzyme were determined in this study: (a) containing Cibacron Blue, a potent competitive inhibitor with respect to NAD(P)H, and the quinonoid compound duroquinone and (b) with NADP<sup>+</sup>.

Although DT-diaphorase is recognized as of considerable therapeutic value in the reductive activation of prodrugs, significant differences exist in the abilities of the enzyme in different species to activate these anti-tumor agents. The rat enzyme is more effective than the human in reducing MMC, EO9, streptonigrin, and also CB1954.<sup>6,13–16</sup> All these compounds are therefore better substrates for the rat enzyme than for the human. The molecular basis for these catalytic differences has been recently investigated by site-directed mutagenesis.<sup>17</sup> Together with data from the crystal structure of the rat enzyme complexed with the triazine dye Cibacron blue,<sup>12</sup> this has led to the suggestion that a tyrosine residue (Tyr104), which is substituted by a glutamine in the human enzyme, plays a critical role in the differences in rates of catalysis. Tyr130A is also predicted to be involved and is positioned close to the nicotinamide moiety of NAD(P)H. A full molecular understanding of these differences and their implications is essential for the design of new and improved substrates that can be more effectively reduced by the human enzyme.

### Results and Discussion

**Overall Structure.** Four independent monomers (one tetramer), each containing a noncovalently bound

\* Address correspondence to Prof. S. Neidle, The Institute of Cancer Research, Chester Beatty Laboratories, 237 Fulham Road, London SW3 6JB, U.K. Tel: 0044 171 352 8133. E-mail: s.neidle@icr.ac.uk.

<sup>†</sup> CRC Biomolecular Structure Unit, ICR.

<sup>‡</sup> Kings College London.

<sup>§</sup> CRC Centre for Cancer Therapeutics, ICR.

	1				50
human	MVGRRALIVL	AHSERTSFNY	AMKEAAAAAL	KKKGWEVVES	DLYAMNFNPI
rat	AVRRALIVL	AHAERTSFNY	AMKEAAVEAL	KKKGWEVVES	DLYAMNFNPL
	51				100
human	ISRKDITGKL	KDPANFOYPA	ESVLAYKEGH	LSPDIVAEQK	KLEAADLVIF
rat	ISRNDITGEP	KDSENFQYPV	ESSLAYKEGR	LSPDIVAEQK	KLEAADLVIF
	101				150
human	QFPLQWFGVP	AILKGWFERV	FIGEFAYTYA	AMYDKGPFRS	KKAVLSITTG
rat	QFPLYWFGVP	AILKGWFERV	LVAGFAYTYA	TMYDKGPFQN	KKTLLSITTG
	151				200
human	GSGSMYSLQG	IHGDMNVILW	PIQSGILHFC	GFQVLEPQLT	YSIGHTPADA
rat	GSGSMYSLQG	VHGDMNVILW	PIQSGILRFC	GFQVLEPQLV	YSIGHTPPDA
	201				250
human	RIQILEGWKK	RLENIWDETP	LYFAPSSLFD	LNFQAGFLMK	KEVQDEEKNK
rat	RVQVLEGWKK	RLETVWEESP	LYFAPSSLFD	LNFQAGFLLK	KEVQEEQKKN
	251		274		
human	KFGLSVGHHL	GKSIPTDNQi	KARK		
rat	KFGLSVGHHL	GKSIPADNQi	KARK		

**Figure 1.** Aligned amino acid sequences of human and rat DT-diaphorase. The differences between the two are highlighted in red.

FAD cofactor molecule, form the asymmetric unit of human DT-diaphorase (Figure 2a). The monomers are arranged as two noncrystallographic physiological dimers, with the active site being at each dimer interface. All four chains have essentially identical structures. Backbone conformations are all equivalent, within experimental error with a rms deviation between them of 0.3 Å. The rms deviation, including side-chain atoms, is 0.4 Å. There is also no significant difference between backbone conformations for the rat and human diaphorases, with an rms deviation of 0.55 Å, using averaged conformations for both.

**FAD Binding Site.** There are no significant differences in the backbone conformations of the active-site residues between the four subunits of the human structure. Almost all side-chain conformations are also conserved. Residues Trp105 and Phe106, which are both conserved, and Gln104 form a pocket around the isoalloxazine moiety. Together with the main chain carbonyl of Leu103, these residues are involved in the stabilization of the FAD prosthetic group via interactions with the flavin rings. The overall geometries of the active site are very similar in both the rat and human structures. The rms deviation between the averaged human and rat backbones for residues 100–165 is 0.4 Å (Figure 2b). In view of the conservation of active-site structures for these two species, we conclude that the binding of the Cibacron Blue and duroquinone molecules in the rat structure has had no significant perturbing effect on the active site. A water molecule was found to be bound close to the active site of the human enzyme, hydrogen-bonded to Trp105 and Glu117. This is distant from the position of the bound duroquinone in the rat structure and thus would have little effect on any drug binding.

The FAD molecule adopts identical conformations in both rat and human structures, although there is a shift in its position in the latter, resulting in the FAD molecule being buried slightly more deeply in the active site. In the rat enzyme residue 104 is a tyrosine, which has been postulated by site-directed mutagenesis experiments to be the key residue responsible for the catalytic differences between the rat and human en-

zymes. A hydrogen bond is formed by a water molecule situated between Tyr104 and a phosphate oxygen of FAD in the rat structure. The absence of this interaction in the human structure, where Tyr104 is replaced by glutamine, directly results in the shift of FAD position. In the human enzyme the flavin is shifted by 0.7 Å with respect to the rat (calculated as a mean of the rms deviations from the rat structure measured in all four monomers). An approximate 0.7 Å shift in position had earlier been suggested;<sup>17</sup> it was then unclear whether this difference is chiefly responsible for the differences in substrate reaction rates between the two enzymes. The phenol ring of Tyr128 adopts a distinct conformation in the two enzymes, possibly as a consequence of the hydrogen bonding to the duroquinone molecule found in the rat structure (see also below). There does not appear to be any other underlying significance to this change in side-chain conformation, or to that at Tyr126. The change at amino acid 130 from threonine (rat) to alanine (human) has not resulted in any backbone changes, contrary to earlier suggestions<sup>17</sup> that this region might exhibit small but significant conformational changes; the rms deviation for the C $\alpha$  atoms of residues 127–130 is 0.1 Å, comparing rat to human.

The active site in both human and rat enzymes is formed by the interface between two protein chains. There are some differences in the shape and overall volume of the human compared to the rat active site, due to changes in some of the hydrophobic residues forming its boundary. Most noteworthy are Val69 and Leu120 in the rat enzyme, which are changed to Ala69 and Phe120 in the human. These substitutions will doubtless influence the size of substrate able to bind in the active site.

**Molecular Modeling of CB1954.** Use of the AFFINITY program within the INSIGHTII molecular modeling package resulted in the location of energetically favorable positions and orientation for the CB1954 drug molecule in each active site, for human and rat DT-diaphorase respectively (Figures 3). In each case, only one orientation for the drug is possible, as a consequence of steric clashes in alternative orientations.

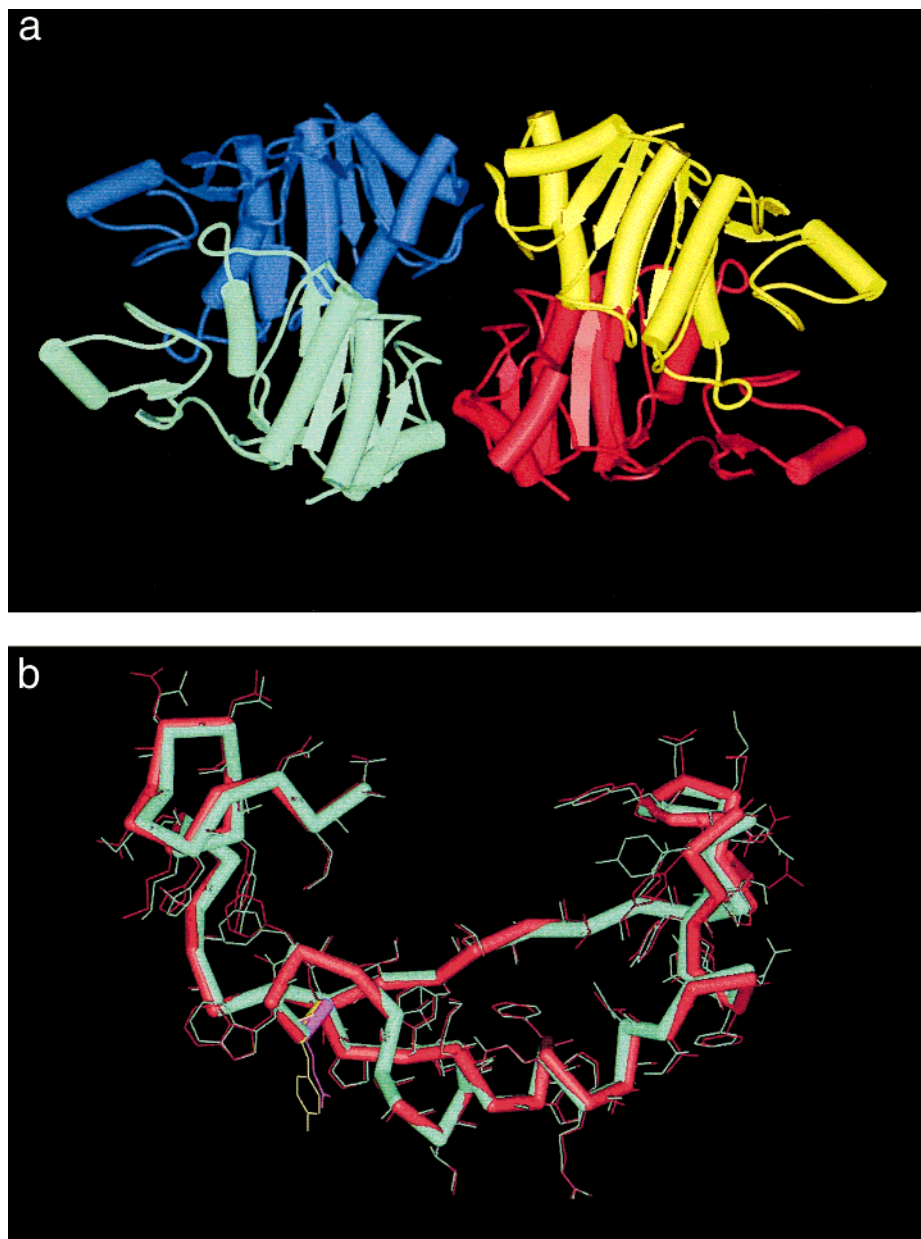


**Figure 2.** (a) The four subunits in the crystal structure of human DT-diaphorase. (b) Superposition of the C $\alpha$  atoms for residues 100–165, for rat and human DT-diaphorase. The rat structure is in cyan and the human in red. The side chain of residue Tyr104 of the rat enzyme is shown in yellow, and Gln104 of the human enzyme is shown in magenta.

The calculated binding energies for both enzyme–drug complexes are closely similar. The van der Waals component energies for the human and rat complexes are  $-54.5$  and  $-54.4$  kcal mol $^{-1}$ , respectively, and the electrostatic components are  $-19.0$  and  $-19.4$  kcal mol $^{-1}$ , giving binding energies of  $-73.5$  and  $-73.8$  kcal mol $^{-1}$ . This result is paralleled by the similarity in low-energy positions for the drug in the two active sites, although there is a small displacement in position due to the change in position of the FAD molecule. The CB1954 molecule is close to the position of the duroquinone molecule observed in the rat crystal structure. The orientations of the aziridine and 4-nitro groups, are predicted by the modeling to be closely similar in the two active sites. We suggest that significant factors in governing the drug position are the close van der Waals contact which the aziridine ring has with the aromatic

ring of Trp105 and the stacking interactions with the planar isoalloxazine ring of the flavin.

The CB1954 molecule in both active sites is indicated by the modeling to participate in hydrogen bonding between side chains and drug substituent atoms (Figure 3). There are some differences in the details of the arrangements. In the model for the rat enzyme–drug complex (Figure 3a) both oxygen atoms, O3 and O4, of the 4-nitro group hydrogen-bond to Tyr126 and Tyr128, from subunit B. There is also a close electrostatic interaction with His161. In the human complex (Figure 3b), Tyr155 is predicted to be 0.4 Å closer to the amide oxygen atom of CB1954. Only Tyr128, in the human complex, is sufficiently close to the 4-nitro group to hydrogen-bond to atom O1 since the side chain of Tyr128 is swung round the CA–CB bond in the human enzyme compared to the rat. This enables Tyr128 to be within hydrogen-bonding distance of the ring nitrogen

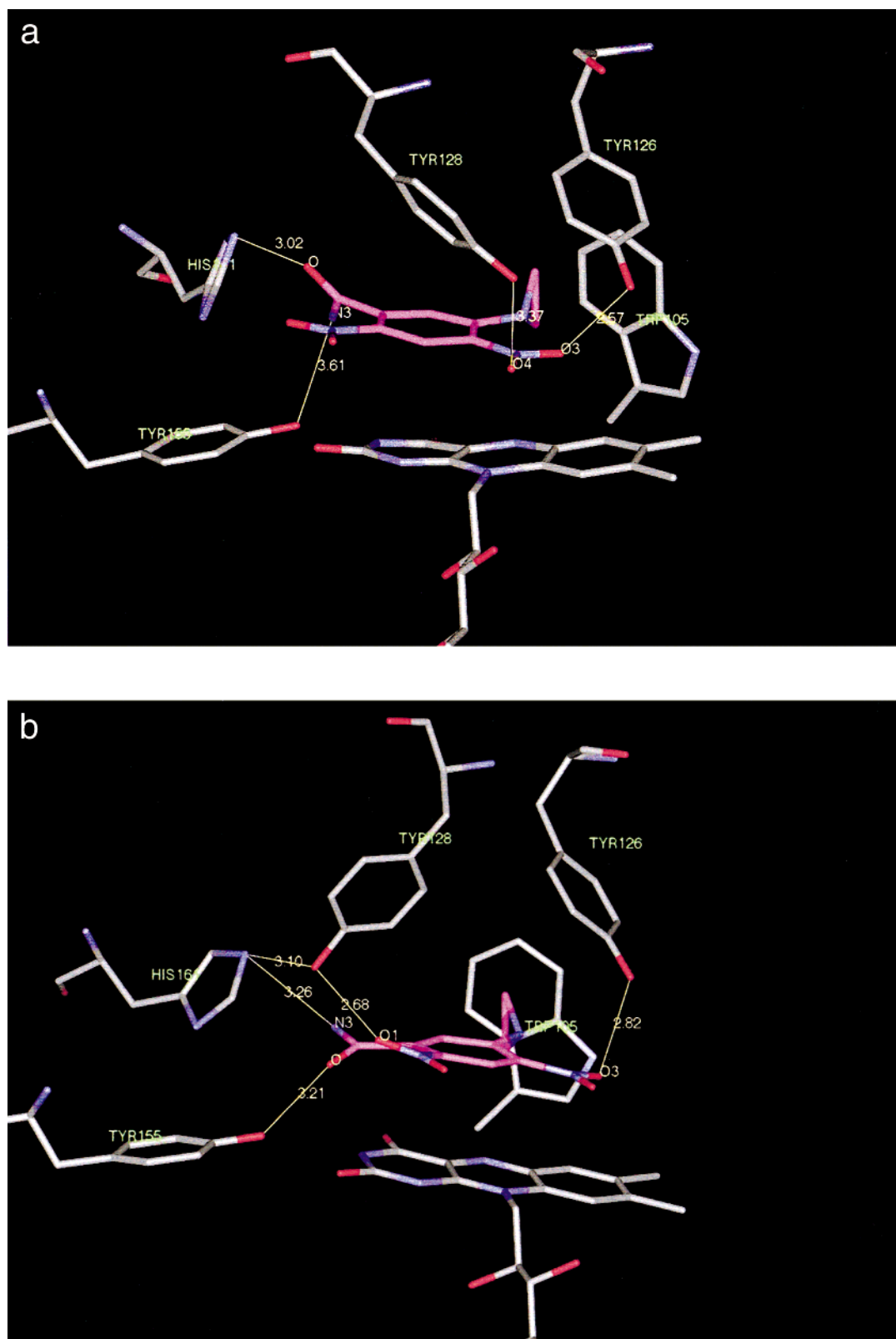


**Figure 3.** (a) Results of the molecular modeling study, showing the CB1954 and FAD molecules bound in the active site of (a) rat and (b) human DT-diaphorase. Only those residues with direct contacts to the drug molecule are shown. Potential hydrogen bonds are shown as thin yellow lines. The carbon atoms of the CB1954 molecule are highlighted in purple. Two views are shown for each active site, looking along and onto the plane of the isoalloxazine moiety of the FAD molecule.

atom of His161, which is now slightly further (3.3 Å) away from the amide group of CB1954 compared to its position in the rat active site.

Although the CB1954 molecule is predicted to be in overall very similar environments in the human and rat

active sites, the differences outlined above may contribute to the observed differences in the drug's rate of two-electron reduction. The postulated mechanism of two-electron transfer<sup>12</sup> involves the transfer of a proton from His161. We note that the net effect of the small

movement in flavin position on going from rat to human is to slightly change the separation between His161 and CB1954, with the drug being closer to His161 in the rat site. We suggest that this small difference may be a factor in facilitating the two-electron transfer, which in the human site may be dissipated through the proximity of Tyr128 to His161. The significance of the hydrogen bonding from the two tyrosine residues 126 and 128 to the 2-nitro position of CB1954 in the rat site is unclear, although it is this nitro group which undergoes nitro reduction by DT-diaphorase to a hydroxylamine.

## Methods

**Expression and Purification.** A sequence containing the cDNA for human DT-diaphorase (a gift from Dr. Anil Jaiswal) was subcloned into plasmid pET11d (Novagen Inc.) and expressed in BL21 (DE3)pLysS cells by induction with IPTG (1 mM) at 37 °C for 10 h. The pelleted cells were resuspended in 50–100 mL of lysis buffer A containing 50 mM Tris-HCl, pH 7.4, 0.15 M NaCl, 2% v/v aprotinin, and the bacterial pellet was disrupted by sonication following freeze/thawing. After centrifugation at 12000g, the cell lysate was treated with 1% poly(ethylenimine) (Sigma) to remove nucleic acids before affinity chromatography on Cibacron Blue using a 5-mL Hi trap column equilibrated in buffer A. Contaminating proteins were eluted by developing a linear gradient over 10 column volumes from 0% to 100% buffer B containing 50 mM Tris-HCl, pH 7.4, 1 M NaCl. DT-diaphorase was eluted with reduced NADH (16 mM) in 1 M Tris-HCl, pH 7.4, containing 0.5 mM KCl and 0.25 M sucrose. Homogeneity was assessed by spectroscopic analysis and SDS-PAGE gels. The specific activity was determined using the menadione assay.<sup>18</sup> The molar extinction coefficients at 272 nm ( $6.65 \times 10^4$ ) and 451 nm ( $1.06 \times 10^4$ ) were used to determine the concentration.<sup>19</sup> The purified protein was concentrated by ultrafiltration and filtered (0.22  $\mu$ m) prior to crystallization.

**Crystallization.** Crystals were grown in sitting drops using the vapor diffusion technique. Equal volumes (4  $\mu$ L) of protein (9.7 mg/mL) in 100 mM sodium phosphate buffer, pH 7.5, were mixed with reservoir solutions containing 25% w/v poly(ethylene glycol) 4000. The nonionic detergent cyclohexyl-propyl- $\beta$ -D-maltoside CYMAL-3 (1  $\mu$ L of 345 mM, CMC 34.5 mM) was added to the droplet. The crystals grew over several weeks as yellow rectangular plates at 18 °C and were predisposed to twinning. Twinning was believed to be responsible for the crystals cracking during substrate-soaking experiments with CB1954 under nonreducing conditions. These experiments were subsequently abandoned. The final refined cell dimensions are  $a = 55.88$  Å,  $b = 57.49$  Å,  $c = 98.77$  Å,  $\alpha = 77.1^\circ$ ,  $\beta = 76.2^\circ$ , and  $\gamma = 86.9^\circ$ . The space group is  $P1$  with two dimers (one tetramer) in the asymmetric unit, assuming an estimated solvent content of 0.47 and using the Matthews parameter  $V_m$ .<sup>20</sup>

**Crystallography.** Intensity data were collected on an R-AXIS-II image-plate system (Molecular Structures Corp.) with Yale/MSO mirrors mounted on a Rigaku RU200 X-ray generator operating at 100 mA and 50 kV. A complete dataset was collected to 2.28 Å at room temperature on a single crystal that had been preirradiated in a synchrotron beam; 110 frames of data (oscillation range 1.2°) were processed and reduced with DENZO and SCALEPACK.<sup>21</sup> A total of 193 332 reflections were measured, which reduced to 46 165 unique reflections (81.5% completeness), with a  $R_{\text{merge}}$  of 0.132. This value is possibly due to crystal decay due to preexposure.

The structure was solved by molecular replacement using the program AMoRe<sup>22</sup> with the structure of the oxidized rat enzyme complexed with Cibacron Blue as the starting model (Protein Data Bank entry code 1QRD). Rigid-body refinement was carried out using the program XPLOR version 3.1, using data to 3.0 Å.<sup>23</sup> Simulated annealing was then carried out on the monomer using strict noncrystallographic symmetry (NCS). The tetramer was internally generated. Strict NCS was then

replaced by restrained NCS. All four monomers of the molecular replacement model, each containing a stoichiometrically bound FAD cofactor, were rebuilt manually using the program O, version 5.10.<sup>24</sup> Further cycles of refinement were carried out on the complete tetramer after map fitting. A bulk solvent refinement was carried out to improve the map and correct for solvent scattering. Data from 2.3–40 Å were included, resulting in an  $R$  of 26% and  $R_{\text{free}}$  of 28.6%. Solvent molecules were included in the final stages of refinement. The final residuals were  $R = 23.2\%$ ;  $R_{\text{free}} = 28.0\%$  with 66 solvent molecules being included. The coordinate data has been deposited in the Protein Data Bank as entry code 1QBG.

**Molecular Modeling.** The structure of CB1954 was built using the INSIGHTII package, and partial charges were calculated with the AM1 semiempirical quantum chemistry module within INSIGHTII. Its structure was closely comparable with that determined by X-ray crystallography.<sup>25</sup> The optimal fit of CB1954 in the active sites of both human and rat DT-diaphorases was determined with the program AFFINITY.<sup>26</sup> Force-field parameters for both drug and protein residues were taken from the CVFF force field<sup>27</sup> within the DISCOVER module of INSIGHTII. The AFFINITY procedure enabled molecular orientation and position for CB1954 to be explored while monitoring electrostatic and van der Waals drug and protein interactions, while enabling drug and side-chain flexibility to be taken into account. Possible starting orientations were chosen by means of a Monte Carlo algorithm. Individual residues were constrained at this initial docking stage. The best drug positions were subjected to 100 steps of unconstrained molecular mechanics minimization. The final ranking order of structures was based on the resulting energy values.

**Acknowledgment.** This work was supported by the Cancer Research Campaign (Program Grant SP1384 to S. Neidle). We are grateful to Prof. Paul Workman for discussions.

## References

- Ernster, L. DT diaphorase – a Historical Review. *Chem. Scripta* **1987**, *27A*, 1–13.
- Riley, R. J.; Workman, P. DT-diaphorase and Cancer Chemotherapy. *Biochem. Pharmacol.* **1992**, *43*, 1657–1669.
- De Long, M. J.; Prochaska, H. J.; Talalay, P. Induction of NAD(P)H:Quinone Reductase in Murine Hepatoma Cells by Phenolic Antioxidants, Azo Dyes and Other Chemoprotectors: A Model System for the Study of Anticarcinogens. *Proc. Natl. Acad. Sci. U.S.A.* **1986**, *83*, 787–791.
- Schlager, J. J.; Powis, G. Cytosolic NAD(P)H: (Quinone Acceptor) Oxidoreductase in Human Normal and Tumour Tissue: Effects of Cigarette Smoking and Alcohol. *Int. J. Cancer* **1990**, *45*, 403–409.
- Knox, R. J.; Friedlos, F.; Boland, M. P. The Bioactivation of CB1954 and its Use as a Prodrug in Antibody-Directed Prodrug Therapy (ADEPT). *Cancer Metastasis Rev.* **1993**, *12*, 195–212.
- Boland, M. P.; Knox, R. J.; Roberts, J. J. The Differences in Kinetics of Rat and Human DT-diaphorase result in a Differential Sensitivity of Derived Cell Lines to CB1954 (5-(Aziridin-1-yl)-2,4-Dinitrobenzamide). *Biochem. Pharmacol.* **1991**, *41*, 867–875.
- Mikami, K.; Naito, M.; Tomida, A.; Yamada, M.; Sirakusa, T.; Tsurua, T. DT Diaphorase as a Critical Determinant of Sensitivity to Mitomycin C in Human Colon and Gastric Carcinoma Cell Lines. *Cancer Res.* **1996**, *56*, 2823–2826.
- Hu, L.-T.; Stamberg, J.; Pan, S.-S. The NAD(P)H:Quinone Oxidoreductase Locus in Human Colon Carcinoma HCT 116 Cells Resistant to Mitomycin C. *Cancer Res.* **1996**, *56*, 5253–5259.
- Robertson, J. A.; Chen, H. C.; Nebert, D. W. NAD(P)H: Menadione Oxidoreductase: Novel Purification of the Enzyme, cDNA, and Complete Amino Acid Sequence, and Gene Regulation. *J. Biol. Chem.* **1986**, *261*, 15794–15799.
- Byron, O.; Mistry, P.; Suter, D. A.; Skelly, J. V. DT-Diaphorase Exists as a Dimer-Tetramer Equilibrium in Solution. *Eur. Biophys. J.* **1997**, *25*, 423–430.
- Chen, S.; Deng, P. S. K.; Bailey, J. M.; Sweiderek, K. M. A Two-domain Structure for the Two Subunits of NAD(P)H Quinone Acceptor Oxidoreductase. *Protein Sci.* **1994**, *3*, 51–57.

- (12) Li, R.; Bianchet, M.; Talalay, P.; Amzel, L. M. The Three-Dimensional Structure of NAD(P)H: Quinone Reductase, a Flavoprotein Involved in Cancer Chemoprotection and Chemotherapy: Mechanism of the Two-Electron Reduction. *Proc. Natl. Acad. Sci. U.S.A.* **1995**, *92*, 8846–8850.
- (13) Siegel, D.; Gibson, N. W.; Prusch, P. C.; Ross, D. Metabolism of Mitomycin C by DT diaphorase: Role in Mitomycin C-Induced DNA Damage. *Cancer Res.* **1990**, *50*, 7483–7489.
- (14) Smitskamp-Wilms, E.; Hendriks, H. R.; Peters, G. J. Development, Pharmacology, Role of DT-Diaphorase and Prospects of Indoloquinone EO9. *Gen. Pharmacol.* **1996**, *41*, 867–875.
- (15) Walton, M. I.; Smith, P. J.; Workman, P. The Role of NAD(P)H: Quinone Reductase (EC 1.6.99.2, DT-Diaphorase) in the Reductive Bioactivation of Novel Indoloquinone Antitumour Agent EO9. *Cancer Commun.* **1991**, *3*, 199–206.
- (16) Beall, H. D.; Mulcahy, T.; Siegel, D.; Traver, R. D.; Gibson, N. W.; Ross, D. Metabolism of Bioreductive Antitumour Compounds by Purified Rat and Human DT Diaphorases. *Cancer Res.* **1994**, *54*, 3196–3201.
- (17) Chen, S.; Knox, R.; Wu, K.; Deng, P. S.-K.; Zhou, D.; Bianchet, M. A.; Amzel, L. M. Molecular Basis of the Catalytic Differences among DT-Diaphorase of Human, Rat, and Mouse. *J. Biol. Chem.* **1997**, *272*, 1437–1439.
- (18) Chen, S.; Hwang, J.; Deng, P. S.-K. Inhibition of NAD(P)H: Quinone Acceptor Oxidoreductase by Flavones: a Structure–Activity Study. *Arch. Biochem. Biophys.* **1993**, *302*, 72–77.
- (19) Knox, R. J.; Boland, M. P.; Friedlos, F.; Coles, B.; Southan, C.; Roberts, J. J. The Nitroreductase Enzyme in Walker Cells that Activates 5-(aziridin-1-yl)-2,4-dinitrobenzamide (CB1954) to 5-(aziridin-1-yl)-4-hydroxylamino-2-nitrobenzamide is a Form of NAD(P)H Dehydrogenase (Quinone) (EC 1.6.99.2). *Biochem. Pharmacol.* **1988**, *37*, 4671–4677.
- (20) Matthews, B. W. Solvent Content of Protein Crystals. *J. Mol. Biol.* **1968**, *33*, 491–497.
- (21) Navaza, J. AmoRe: an Automated Package for Molecular Replacement. *Acta Crystallogr.* **1994**, *A50*, 795–800.
- (22) Otwinowski, Z. Data Collection and Processing. In *Proceedings of the CCP4 Study Weekend*; Sawyer, L., Isaacs, N., Bailey, S., Eds.; 1993.
- (23) Brünger, A. T. *XPLOR Version 3.1*; Yale University Press: New Haven, CT, 1993.
- (24) Jones, T. A.; Zou, J.-Y.; Cowan, S. W.; Kjeldgaard, M. Improved Methods for the Building of Protein Models in Electron Density Maps and the Location of Errors in these Models. *Acta Crystallogr.* **1991**, *A47*, 110–119.
- (25) Iball, J.; Scrimgeour, S. N.; Williams, B. C. The Crystal and Molecular Structure of 2,4-dinitro-5-ethyleneiminobenzamide. *Acta Crystallogr.* **1975**, *B31*, 1121–1123.
- (26) Luty, B. A.; Wasserman, Z. R.; Stouten, P. F. W.; Hodge, C. N.; Zacharias, M.; McCammon, J. A. A Molecular Mechanics/Grid Method for Evaluation of Ligand–Receptor Interactions. *J. Comput. Chem.* **1995**, *16*, 454–464.
- (27) Dauber-Osguthorpe, P.; Roberts, V. A.; Osguthorpe, D. J.; Wolff, J.; Genest, M.; Hagler, A. T. Structure and Energetics of Ligand Binding to Proteins: E. coli Dihydrofolate Reductase-trimethoprim, a Drug-receptor System. *Proteins* **1988**, *4*, 31–47.

JM991060M